Journal of Ultrafine Grained and Nanostructured Materials
https://jufgnsm.ut.ac.ir
Vol. 54, No.2, December 2021, pp. 121-130
Print ISSN: 2423-6845 Online ISSN: 2423-6837
DOI: 10.22059/jufgnsm.2021.02.01

Effect of SiC nanoparticles addition on densification of commercially pure Al and 5252 Al powder compacts

Mohammad Moazami-Goudarzi[1], Farshad Akhlaghi*[*,2]

[1]Department of Materials Engineering, Science and Research Branch, Islamic Azad University, Tehran, Iran;
[2]School of Metallurgy and Materials Engineering, College of Engineering, University of Tehran, Tehran, Iran.

Recieved: 1 October 2021; Accepted: 23 October 2021
**Corresponding author email: fakhlagh@ut.ac.ir*

ABSTRACT

One of the main challenges in processing of metal matrix nanocomposites through the powder metallurgy method is achieving a dense compact with minimum internal porosity. Pores act as stress risers and deteriorate the mechanical properties of nano-materials. In the present investigation, powder mixtures of commercially pure Al (CP-Al) and 5252 Al alloy reinforced with nanometric SiC particles (0-7 wt.%) were produced by in situ powder metallurgy (IPM) method. These powders were consolidated through cold compaction, sintering and hot extrusion processes and subjected to density measurements, microstructural studies and thermal analysis. Microstructural studies showed that SiC nanoparticles formed a continuous network around the CP-Al powders, restricting effective densification during the cold compaction stage. This network was also shown to prevent metal-to-metal contact during sintering, especially at higher SiC contents. Therefore, a remarkable decrease in the sintered relative density was observed with increasing SiC contents in the CP-Al/SiC compacts. However, in the 5252 Al/SiC composite powders, the SiC nanoparticles embedded within the alloy matrix during the IPM process. As a result, a more homogeneous SiC particle distribution was attained. This led to enhanced cold densification and improved sinterability compared with those of CP-Al/SiC powder mixture. Besides, the presence of Mg in the 5252 alloy matrix was effective in reducing the oxide film covering the Al particles. The differential scanning calorimetry (DSC) revealed the formation of liquid phase during the sintering of 5252 Al/SiC powder compacts. As a result, mass transfer promoted through the liquid phase sintering enhancing densification. However, improved densification was obtained after hot extrusion of the nano-SiC reinforced composites. Results showed that the pressure required for extrusion increased with increasing SiC content. This was attributed to the enhanced redundant work induced by SiC particles.

Keywords: *Al/SiC nanocomposite, Cold densification, Liquid phase sintering, Hot extrusion*

1. Introduction

Aluminum matrix nanocomposites have been reported to offer superior mechanical properties [1, 2]. Powder metallurgy is the main processing route for fabricating this new generation of metal matrix composites (MMCs). In traditional powder metallurgy, the matrix alloy powder is mixed with nanometric ceramic reinforcements [3]. In novel methods such as mechanical milling [4] and in-situ powder metallurgy (IPM) [5], the nanosized reinforcements are embedded within the metallic matrix powders. The IPM method was initially developed for processing of Al matrix composites reinforced with either micron-sized graphite

[6] or alumina [7] particles. For the production of nanocomposite powder by IPM method, relatively coarse micrometric ceramic particles; as solid atomizing media; are usually added to the slurry containing nanosized reinforcements. An impeller stirs the mixture mechanically. The melt disintegration occurs by kinetic energy transferring from the stirrer to the molten metal via the solid media. The resultant liquid droplets are converted to metallic powders after solidification. The coarse ceramic particles are then sieved out from the mixture of metallic powder and nanosized reinforcements. This results in a uniform distribution of reinforcing particles within the matrix alloy [8]. However, full densification is required to ensure enhanced mechanical properties.

Cold compaction is usually the first step of consolidation in powder metallurgy, followed by sintering, hot extrusion, or other secondary operations. The primary purpose of compaction is to produce a green compact with sufficient strength to withstand further handling operations. The important processes involved in powder compaction include powder rearrangement, plastic deformation, and fragmentation (for brittle materials). While densification occurs mainly in the cold consolidation step, secondary processing treatments are inevitable to produce a fully dense material [9].

Sintering is a widespread densification process in traditional powder metallurgy. It is carried out by heating the green compact up to a temperature below the main constituent's melting point, leading to the bonding of adjacent particles in the powder mass. The driving force of sintering is the reduction of surface energy. From a geometrical point of view, sintering is usually divided into three stages. First bonds or necks growth occurs in the initial stage of sintering. In the intermediate stage, neighboring sinter necks grow sufficiently large to overlap each other. The final stage of sintering includes pore rounding and results in high densities [10]. For the cold-pressed aluminum powders at 300 to 400 MPa, the sintered density of about 95 to 97 percent of theoretical value can be obtained [11]. However, the addition of ceramic particles into metallic powders hinders densification of the powder compact in cold compacted [12] and sintered [13] states. This reduced densification is more evident for nanocomposites as compared with microcomposites [14]. On the other hand, the addition of magnesium to aluminum and sintering in the presence of a liquid phase is reported to enhance the sinterability of powder-processed aluminum products [15].

In the hot extrusion processing method, hot compaction and hot mechanical working are combined to produce a fully dense product. The extrusion process offers the ability to form wrought structures from powders without the need for sintering. This is particularly useful in the case of aluminum alloys in which sintering is difficult due to the presence of an oxide film on the powder particle surfaces. In addition, extrusion improves the distribution of reinforcements in the aluminum matrix [16]. To achieve complete densification by extrusion, extrusion ratios of more than 9:1 have been recommended [11].

In the present investigation, the effect of Mg and SiC addition on densification of aluminum powders in different consolidation stages involved in PM, i.e. cold compaction, sintering, and hot extrusion are studied.

2. Experimental

The IPM method was employed for the fabrication of two different types of powder mixtures. The chemical compositions of the commercially pure Al (CP-Al) and 5252 Al alloy, used as the matrix materials in the present study, are given in Table 1. Different contents (0-7wt.%) of SiC particles (60 nm) were used as the reinforcing phase. Detailed information about IPM processing of powder mixtures containing SiC particles is reported elsewhere [17]. A Cilas 1064 laser particle size analyzer was utilized for measuring the average particle size. To determine the solidus and liquidus points of the matrix alloys, the powder samples were also analyzed by differential scanning calorimetry (DSC) using a Liuscis HDSC L62H1550 calorimeter. The DSC analysis was carried out in an argon atmosphere with a heating rate of 15°C/min. Then, powder mixtures were uniaxially cold pressed at 600 MPa in

Table 1- Chemical composition (wt.%) of the matrix powders

Matrix alloy	Si	Fe	Cu	Mn	Mg	Zn	Al
CP-Al	0.050	0.068	<0.001	0.021	<0.001	0.002	99.84
Al-Mg (5252)	0.044	0.068	0.004	0.018	2.47	0.004	balance

a cylindrical steel die. The green compacts were then consolidated by sintering or hot extrusion. Sintering was performed in a tubular furnace at 620°C under an argon atmosphere for 90 min at a heating rate of 15°C/min. Hot extrusion was carried out at a ram speed of 36 mm/min on Al-2.5Mg (5252) based compacts at 500°C. The extrusion ratio was 11:1 and the colloidal graphite powder in acetone was applied as lubricant to the internal surface of the die before heating up to extrusion temperature. The densities of green compacts as well as sintered or extruded samples were measured using Archimedes' method. The morphology and microstructure of powders and sintered compacts were examined by a CamScan MV2300 scanning electron microscope (SEM).

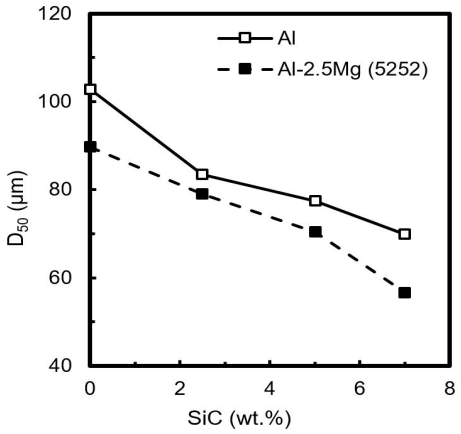

Fig. 1- Effect of nanosized SiC particles addition on the size of produced powders.

3. Results and discussion

3.1. Characteristics of powders

Fig. 1 shows the effect of SiC weight percentage on the mass median diameter (D_{50}) of produced powders. The increased SiC content resulted in the production of finer powders in both CP-Al and 5252 Al-based powder mixtures. Generally, the size of powders produced by the IPM method is affected by processing parameters and chemical composition of the melt [18]. The reduced particle size with increased SiC content can be attributed to the considerable increase in the surface of solid particles (i.e. by increased SiC addition) involved in the IPM process. In addition, an increase in the Mg content of the matrix alloy from 0 in CP-Al to 2.5 wt.% in 5252 Al alloy resulted in a reduction in D_{50} values, indicating that finer powders were produced, regardless of the SiC content of powders. The noticeable effect of Mg on the atomization efficiency of Al melt is the main reason for production of finer powders. This, in turn, changes the morphology of powders containing different Mg contents. Principally, the morphology of powders produced via the IPM method is only influenced by their size [8]. Large powders are spherical and small powders are irregular in shape. The main mechanisms affecting the size and morphology of generated powder particles were explained in the literature [8, 17].

Another difference between CP-Al and 5252 Al-based powders was detected using metallographic investigations. Figs. 2a and b, illustrate the

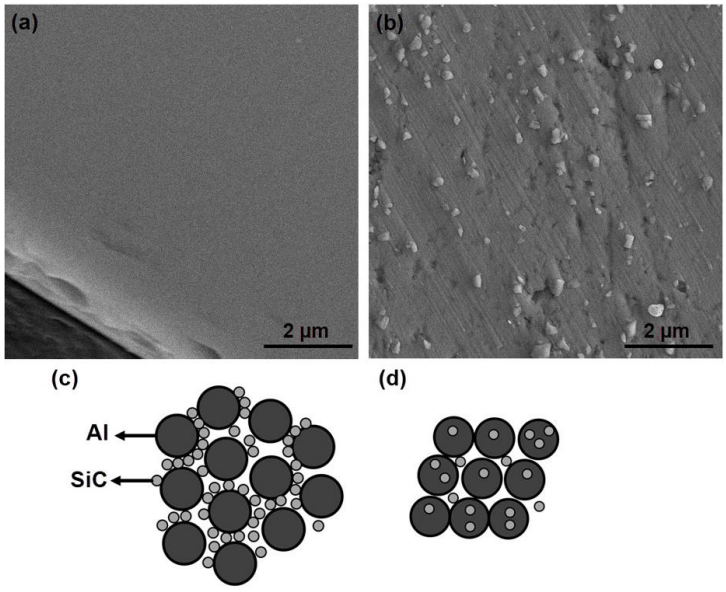

Fig. 2- SEM micrographs from the cross-section of CP-Al/5wt.% SiC (a) and 5252 Al/5wt.% SiC (b) powders and schematic illustration of them, respectively (c) and (d).

microstructure of CP-Al and 5252 Al-based powders, respectively, both containing 5 wt.% SiC particles. While CP-Al powders contain no SiC particles, 5252 Al powders are reinforced by SiC nanoparticles. Our previous study [18], focusing on incorporating SiC within the aluminum matrix, showed that at least 1 wt.% Mg in Al was required to embed SiC nanoparticles into the matrix alloy. These results were attributed to the effect of Mg as an enhancive wetting agent for SiC particles. In the case of 5252 Al-based powders, as depicted schematically in Fig. 2d, each powder is a composite powder containing nanosized reinforcements. However, the processing of CP-Al/nano-SiC powders via the IPM method resulted in generating a mixture of free SiC nanoparticles or their agglomerates accompanied with monolithic CP-Al powders. In this series of powders, as observed schematically in Fig. 2c, SiC nanoparticles are distributed between CP-Al powders representing a conventional mixture of metallic powders with nanometric reinforcements.

The DSC curves of Al and 5252 Al alloy are shown in Fig. 3. For both matrix materials, the DSC traces showed an endothermic peak. The first deviation from the baseline determines the onset temperatures for melting. For the commercially pure Al, the onset is sharp and the DSC curve is almost linear after the onset. The peak temperature on the DSC plot indicated the liquidus temperature of the matrix alloy. The results of DSC analysis together with solidus and liquidus temperatures of Al matrix alloys reported in the literature are summarized in Table 2. The onset temperatures for melting of both matrix materials are lower than their reported thermodynamic quantities, i.e. solidus point. Indeed, during heating, the matrix alloys began to partially melt below the equilibrium solidus point. This onset temperature of partial melting is usually called the incipient melting point. The incipient melting normally occurs because of the microsegregation of solute elements at grain boundaries or interdendritic regions [19]. In fact, the lower onset temperatures of melting obtained for the matrix alloys compared with the reported solidus values (Table 2) can be attributed to the existence of composition gradients within individual phases in the alloy microstructure due to the non-equilibrium solidification.

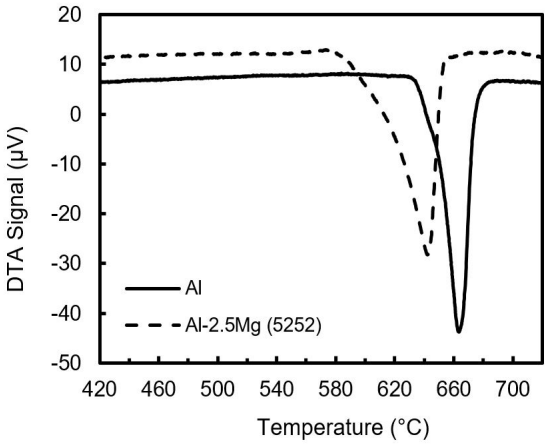

Fig. 3- DSC curves for commercially pure Al and 5252 Al alloy.

3.2. Cold compaction and sintering

Fig. 4 shows that both green and sintered density of powder samples decreased with increasing SiC content. The decrease in green density of all specimens with increased SiC content (Fig. 4a) can be attributed to the decreased particle rearrangement which is the first step of densification in cold compaction of powders [8]. This is a consequence of an increased percentage of irregularly shaped particles due to the generation of finer powders leading to increased friction between adjacent powder particles. In addition, in the presence of a non-deformable ceramic phase, i.e. SiC particles, the soft metallic powders must undergo additional deformation to achieve a given amount of densification. This results in the reduction of compressibility with increased SiC percentage. In fact, at a constant compacting pressure, the plastic deformation, i.e. second stage of densification, is retarded by the addition of nanosized SiC particles.

The inferior densification of the conventional mixture of metal and ceramic particles, i.e. Al-based powder mixture, is attributed to the formation of a continuous network of hard SiC particles. This network supports a portion of the applied pressure and reduces the

Table 2- Characteristic temperatures (°C) of matrix alloys obtained from DSC analysis

Matrix alloy	Onset temperature for melting	Peak temperature	Reported Solidus temperature [20]	Reported Liquidus temperature [20]
CP-Al	634	663	646[a]	657*
Al-Mg (5252)	580	642	607	649

[a] Characteristic temperatures of AA 1060 alloy are adopted.

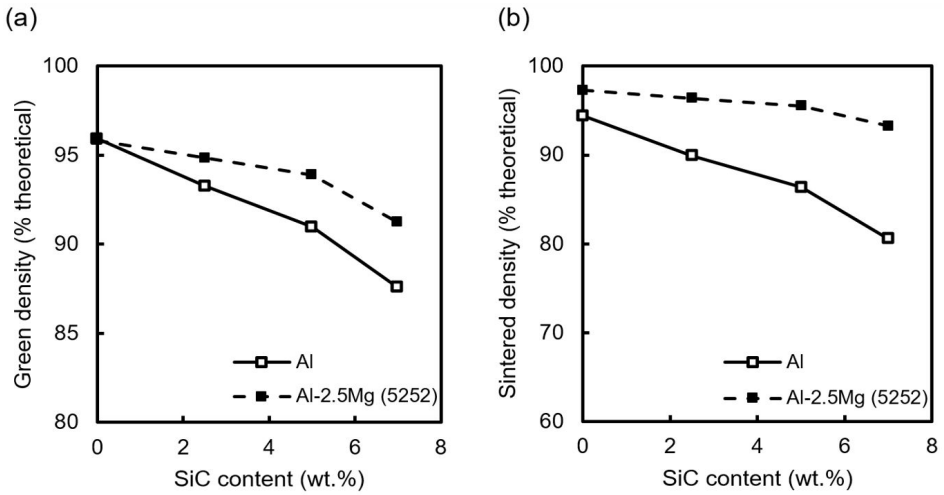

Fig. 4- Green density (a) and sintered density (b) of samples versus nanosized SiC contents.

transmitted load to the soft plastic particles.

Fig. 4b shows that while the sintered density of both Al and 5252 Al-based samples decreased with increasing SiC content, this reduction is more prominent for the former. This decreased sintered density is mainly due to the reduced relative density of green compacts containing higher weight percentages of SiC nanoparticles (Fig. 4a). Low values of green density result in reduced contact points between powder particles and, consequently deterirate the sintering process. A lower green density indicates the increased surface of porosities within compacts, and consequently imposes a greater driving force for sintering. Therefore, it is anticipated that the compacts with lower relative green density exhibit higher density variations during sintering.

In addition, Fig. 4b shows that the sintered density of 5252 Al matrix samples at a given SiC content is higher than that of its CP-Al-based counterpart. This is partially due to superior green densities of 5252 Al-based compacts at any SiC content. However, while the green density of the monolithic 5252 Al compact was almost equal to that of Al, the sintered density of the former is higher. This suggests that another parameter, apart from the green density, affects the densification of the sintered compacts. To exclude the effect of green density on sintered density values, the densification parameter was used as follows [21]:

$$\psi = \frac{\rho_s - \rho_g}{\rho_{th} - \rho_g} \quad (1)$$

where ρ_s, ρ_g, and ρ_{th} are sintered, green, and theoretical density values, respectively. The

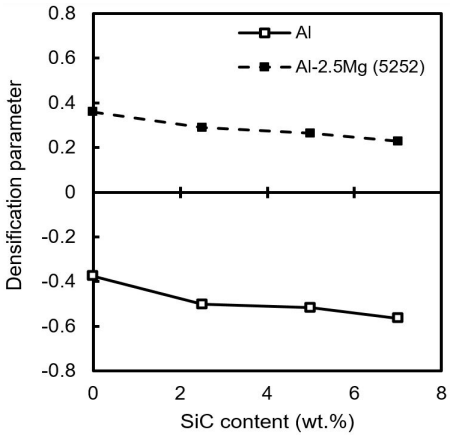

Fig. 5- Densification parameter versus SiC content of samples.

densification parameter is a measure of sinterability of powder compacts. A positive densification parameter indicates shrinkage of the compact during sintering, while a negative value represents expansion. The variations of densification parameter with SiC content in CP-Al and 5252 Al-based compacts are presented in Fig.5. The densification parameter for monolithic CP-Al and CP-Al/SiC compacts were negative, indicating that their density was reduced by sintering. In fact, a growth in compact dimensions, i.e. swelling, occurred during sintering. In CP-Al/SiC compacts, the sintering temperature (620°C) was far below the melting point of the matrix (i.e. 634°C from Table 2), and thereby no liquid phase has been formed during sintering. Therefore, swelling may be attributed to the expansion of trapped gases in closed pores.

The oxide film (Al_2O_3) covering the surface of aluminum powders acts as a severe barrier for solid-state sintering [22]. This oxide layer reduces the diffusion rate and prevents metal-to-metal contact, which is essential for subsequent mass transfer. In fact, the problem caused by the oxide coating is to such an extent that solid-state sintering is considered as an impractical method for densification of pure Al [23]. A typical micrograph from a cross-section of monolithic CP-Al compact after sintering is shown in Fig. 6a. The existence of primary boundaries of powder particles in most areas signifies that even necking (the initial stage of sintering) has not been occurred. The formidable oxide film has retarded the diffusion process and therefore hindered different stages of solid-state sintering. Consequently, sintering was not completed and resulted in a compact with a reduced density.

Fig. 5 also shows that the sinterability of CP-Al-based compacts decreased significantly with increasing SiC content. The SEM micrograph of the cross-section of the sintered Al/5wt.% SiC compact as shown in Fig. 6b, reveal intact primary boundaries of powder particles in all points. The boundaries between individual powders seem to be broader and more significant, as compared with the compact free from SiC particles (Fig. 6a). This microstructure virtually represents an unsintered product. As noted earlier, in the conventional mixture of CP-Al and SiC powders, nanosized SiC particles form a percolating network between aluminum powders preventing metal to metal contact (Fig. 2c). As a result, the available path for diffusion is significantly restricted, and the sinterability decreases. The extent of this network increases with the increased SiC content of the powder compact, resulting in a reduction in the densification parameter (Fig. 5). Similarly, Dabhade et al. [24] reported the reduced densification of Ti powder compact with the addition of TiN nanoparticles. On the other hand, the increased content of SiC particles resulted in the production of finer powders (Fig. 1). This, in turn, increased the overall percentage of irregularly shaped powders within the mixture [8, 17]. Finer powders have a greater pore/solid interfacial area producing a greater driving force for sintering. In addition, the available paths for diffusion increase with decreased particle size, inducing enhanced surface diffusion. Moreover, the greater interparticle contact area also intensifies volume diffusion. In addition, the increased irregularity of particle shape enhances the internal surface area and promotes sintering. However, the results show that the effect of addition of SiC nanoparticles on the reduction of sintered density arising from the formation of particle networks dominates its positive effects resulting from the particle size reduction.

According to the sinterability diagram (Fig. 5), unlike Al-based compacts which expanded by sintering, the densification parameter of samples containing 2.5wt.%Mg (5252 Al-based samples) was positive, indicating shrinkage of the compacts. This implies a change in the sintering mechanisms. The presence of a liquid phase at temperatures higher than 580°C during heating of 5252 Al compact was clearly confirmed by the results of DSC analysis (Table 2). For the 5252 Al-based compacts, sintering at 620°C is of supersolidus liquid phase sintering type. The improved sinterability of aluminum powders with the addition of 2.5wt.%

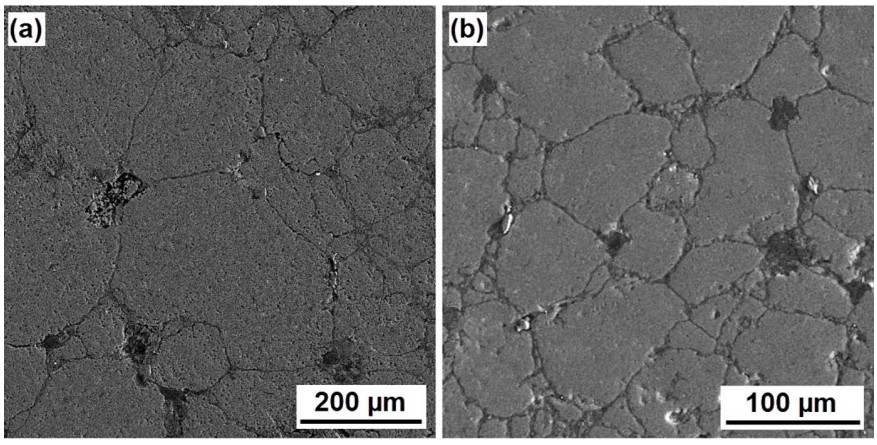

Fig. 6- SEM image from the cross-section of sintered CP-Al (a) and CP-Al/5wt.%SiC (b) compacts.

Mg can therefore be attributed to the sintering events occurred in the presence of the liquid phase. It is generally agreed that the successful sintering of aluminum powders can only be achieved by formation of a liquid phase, breaking up the oxide film on aluminum powders [25]. Schaffer et al. [22] reported that an essential requirement for effective liquid phase sintering is a wetting liquid. Molten aluminum does not wet aluminum oxide at temperatures around the melting point of the aluminum. The wetting angle between Al and $Al_2O_{3,}$ even at 900 °C is more than 90°, and the wetting is not anticipated. However, magnesium is a reactive element and the free energy of its oxide formation is more negative than that of aluminum oxide. Therefore, magnesium can react with aluminum oxide and reduce it. Lumley et al. [26] developed the above discussion and proposed the following reaction:

$$3Mg + 4Al_2O_3 \longleftrightarrow 3MgAl_2O_4 + 2Al \quad (2)$$

The formation of $MgAl_2O_4$ is accompanied by a volume change and creation of shear stresses resulting in disruption of the oxide film. As a result, diffusion, wetting, and sintering occur.

Fig. 7a displays the SEM micrograph from the cross-section of the sintered 5252 Al compact. As observed, the boundaries between particles have been eliminated due to the neck formation. Pores are closed, indicating that the complete sintering process, i.e. up to the final stage, has been occurred. As discussed earlier, this can be attributed to the ability of magnesium to improve the wetting between molten aluminum and alumina and its high tendency to absorb oxygen leading to reduction of the oxide coating covering aluminum powders. Therefore, direct metal-to-metal contact occurs due to the elimination of the oxide coating. Accordingly, liquid phase sintering contributes in the sintering process. During heating, when the sintering temperature exceeds the eutectic temperature, i. e. 449°C [27], the liquid eutectic forms which leads to swelling of the compact [28]. DSC analysis (Table 2) showed that the incipient melting point of the used 5252 Al powders was 580°C. Afterward, with sintering at 620°C, the eutectic liquid diffuses into the pores and fills them, resulting in shrinkage of the compact. The results show that the produced shrinkage compensates for swelling arising from the formation of eutectic liquid or the expansion of entrapped gases. Therefore, the sintered density of all the 5252 Al-based compacts are higher than those of their green counterparts, and their corresponding densification parameters are positive (Figs. 4 and 5).

The SEM micrograph from the cross-section of the sintered 5252 Al/5wt.% SiC compact (Fig. 7b) confirms that the individual composite powders are bonded together, indicating that the sintering has been successful as compared with the compact containing no magnesium (Al/5wt.%SiC compacts shown in Fig. 6b). However, it includes higher porosity in comparison with monolithic 5252 Al compact (Fig. 7a). Consistent with microstructural results, the sinterability diagram (Fig. 5) shows that the densification parameter decreased with increased SiC content. However, in this case, the detrimental effect of SiC addition on sintered density is alleviated compared with CP-Al-based samples. This is mainly because most nanosized SiC particles are embedded within 5252 Al powders,

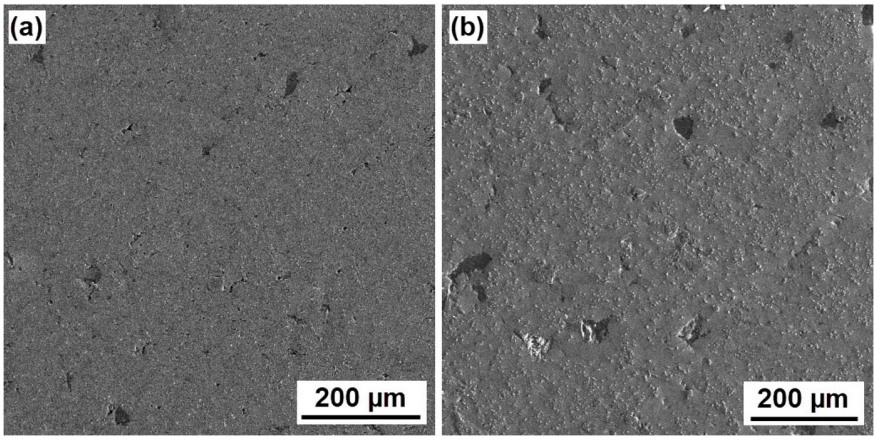

Fig. 7- SEM image from the cross-section of sintered 5252 Al (a) and 5252 Al/5wt.% SiC (b) compacts.

preventing the formation of a continuous network of ceramic particles between metallic powders (Figs. 2 b and d). Li et al. [29] reported that the amount of extra liquid phase needed for successful supersolidus liquid phase sintering of metal matrix composites increased with increased clustering of reinforcement particulates. Accordingly, with increased SiC content accompanied with more clustering, the reduced densification of 5252 Al compacts sintered at a constant temperature (and consequently constant liquid phase) is anticipated. On the other hand, the decreased particle size and increased irregularity arose from the addition of SiC particles, promote sintering. In addition, hard reinforcements are reported to induce a stress field in the aluminum matrix which might enhance diffusion during sintering resulting in increased densification [28]. However, our results showed that those mechanisms that reduced sinterability predominated over those that enhanced densification. Similar results on reduced densification of aluminum powders due to the addition of alumina nanoparticles are reported by Razavi-Tousi et al. [14]. Asgharzadeh and Simchi [30] also reported that the addition of more than 9 vol.% micrometric SiC particles into Al 6061 powders resulted in reduced densification during sintering.

3.3. Hot extrusion

The increased extrusion pressure with SiC content for 5252 Al compacts is shown in Fig. 8. The extrusion pressure is affected by the work needed for homogeneous deformation, friction work, and redundant deformation [31]. Theoretically, the pressure P needed to extrude a compact through a die is expressed as [11]:

$$P = a + b \ln R \quad (3)$$

where the term a refers to redundant work (non-uniform deformation) and b relates to homogeneous work at the extrusion ratio of R. Sheppard et al. [32] reported that the redundant work in powder extrusion includes continuous breaking and rewelding of particles during deformation. They showed that for the powder compact, the redundant work is the major proportion of the total energy required for deformation and contributes to the construction of a coherent material, eliminating the need for any sintering operation.

While temperature, strain rate, and deformation were constant during the extrusion of all the 5252 Al compacts with different SiC contents, redundant work was inconstant. The enhanced extrusion pressure with SiC content (Fig. 8) can be mainly attributed to the increased redundant work involved in the extrusion process. As discussed earlier, the size and morphology of individual Al powders generated during the IPM process respectively decrease and become more irregular with increased SiC particles, both promote the increased total surface area of the powders. Therefore, welding-breaking-rewelding cycles during extrusion of the compacts intensify with increased SiC content, resulting in an increased redundant work. The increased hardness of 5252 Al powders with increased incorporated SiC nanoparticles may be another reason for increasing extrusion pressure with SiC content. Fogagnolo et al. [33] showed that the effect of surface area on extrusion pressure was more significant than that of the hardness of powders. They also found no relation between green density and the pressure required for extrusion of AA6061/AlN composite powders prepared by mechanical alloying.

Figure 9a shows the relative density of extruded 5252 Al samples containing different amounts of SiC particles. The maximum value (99.6%) was attained for the non-reinforced monolithic 5252 Al alloy. The relative density of composite samples reduced slightly with increased SiC content reaching the value of 98.9% for the sample containing 7 wt.% SiC. Balog et al. [34] reported similar values for relative density of Al/Al_2O_3 nanocomposites fabricated by an extrusion ratio

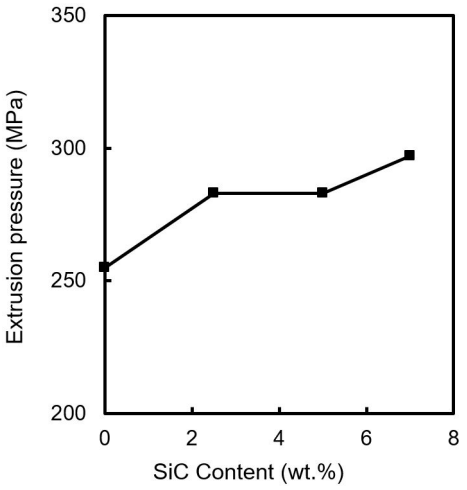

Fig. 8- Extrusion pressure versus SiC content for 5252 Al compacts.

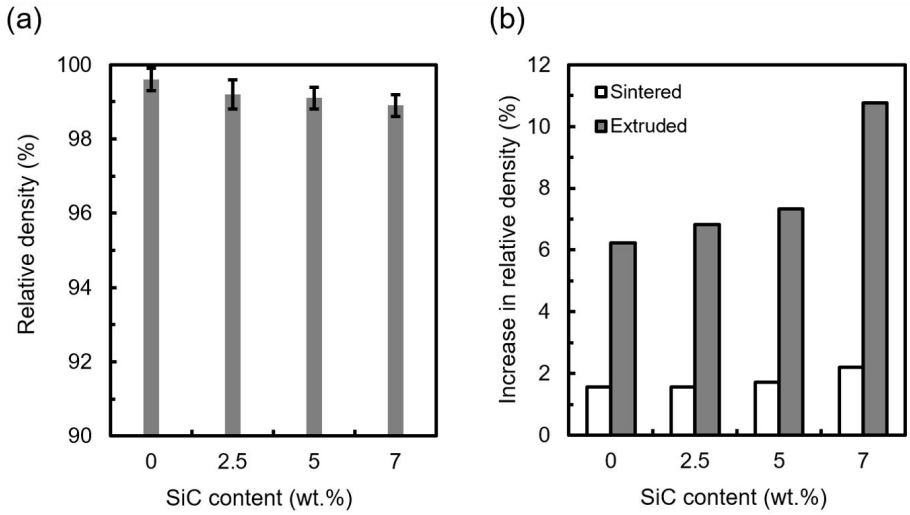

Fig. 9- Effect of SiC contents in 5252 Al samples on (a) relative density of extruded samples and (b) percentage of increase in relative density of sintered and extruded samples as compared with their green counterparts.

of R=11:1. Fig. 9b compares the changes in relative density of green samples gained by sintering and extrusion operations. In both consolidation methods, the percentage of increased relative density enhanced with increased SiC content. This is attributed to the lower green density of powder compacts containing higher SiC contents (Fig. 3a). However, a considerable increase in relative density was attained by hot extrusion as compared with sintering. In addition, the differences between the values of extruded and sintered samples increased with SiC content, indicating that extrusion is a powerful method for consolidation of composite powder compacts. This is mainly due to the severe shear strains involved in the extrusion contributing in enhanced joining of different powder particles at high temperatures.

4. Conclusions

The densification of powder mixtures containing aluminum and nanosized SiC particles was found to be influenced by the type of distribution of SiC particles within powder mass. The enhanced densification was achieved when SiC particles were embedded within 5252 Al matrix alloy powders containing about 2.5wt.% Mg. A continuous percolating network of SiC particles around the CP-Al powders, restricted effective densification by supporting a substantial portion of the applied pressure in cold compaction. It also prevented metal-to-metal contact, which was necessary for successful sintering. The improved sinterability of 5252 Al/SiC compacts as compared with that of CP-Al/SiC ones is also attributed to the effect of magnesium on enhansing liquid phase sintering of aluminum powders.

In all the consolidation steps i.e. cold compaction, sintering and hot extrusion, the increased SiC content deteriorated the densification of both 5252Al powders with embedded SiC particles and CP-Al powders with free SiC particles. However, this effect was minimal in the hot extrusion process. The increased extrusion pressure with increased SiC content attributed to the enhanced redundant work required for welding, breaking and rewelding of powder particles.

At the processing conditions employed in the present study, hot extrusion of 5252 Al/SiC green composite samples with different SiC loadings resulted in significantly more densified samples as compared with their sintered counterparts.

References

1. Ceschini L, Dahle A, Gupta M, Jarfors AEW, Jayalakshmi S, Morri A, et al. Mechanical Behavior of Al and Mg Based Nanocomposites. Aluminum and Magnesium Metal Matrix Nanocomposites: Springer Singapore; 2017. p. 95-137.
2. Prasad Reddy A, Vamsi Krishna P, Rao RN. Mechanical and Wear Properties of Aluminum-Based Nanocomposites Fabricated through Ultrasonic Assisted Stir Casting. Journal of Testing and Evaluation. 2020;48:3035-56.
3. Prasad Reddy A, Vamsi Krishna P, Narasimha Rao R, Murthy NV. Silicon Carbide Reinforced Aluminium Metal Matrix Nano Composites-A Review. Materials Today: Proceedings. 2017;4(2):3959-71.
4. Tang F, Hagiwara M, Schoenung JM. Microstructure and tensile properties of bulk nanostructured Al-5083/SiCp composites prepared by cryomilling. Materials Science and Engineering: A. 2005;407(1-2):306-14.

5. Moazami-Goudarzi M, Akhlaghi F. Effect of nanosized SiC particles addition to CP Al and Al–Mg powders on their compaction behavior. Powder Technology. 2013;245:126-33.
6. Akhlaghi F, Zare-Bidaki A. Influence of graphite content on the dry sliding and oil impregnated sliding wear behavior of Al 2024–graphite composites produced by in situ powder metallurgy method. Wear. 2009;266(1-2):37-45.
7. Pournaderi S, Akhlaghi F. Wear behaviour of Al6061-Al2O3 composites produced by in-situ powder metallurgy (IPM). Powder Technology. 2017;313:184-90.
8. Moazami-Goudarzi M, Akhlaghi F. Effect of SiC Nanoparticles Content and Mg Addition on the Characteristics of Al/SiC Composite Powders Produced via In Situ Powder Metallurgy Method. Particulate Science and Technology. 2013;31(3):234-40.
9. Peng K, Pan H, Zheng Z, Yu J. Compaction behavior and densification mechanisms of Cu W composite powders. Powder Technology. 2021;382:478-90.
10. Felege GN, Gurao NP, Upadhyaya A. Microstructure, microtexture and grain boundary character evolution in microwave sintered copper. Materials Characterization. 2019;157:109921.
11. ASM Handbook, Vol. 7, Powder metal technologies and applications. USA: ASM International; 1992.
12. Martin LP, Hodge AM, Campbell GH. Compaction behavior of uniaxially cold-pressed Bi–Ta composites. Scripta Materialia. 2007;57(3):229-32.
13. Abenojar J. Atmosphere influence in sintering process of stainless steels matrix composites reinforced with hard particles. Composites Science and Technology. 2003;63(1):69-79.
14. Razavi-Tousi SS, Yazdani-Rad R, Manafi SA. Effect of volume fraction and particle size of alumina reinforcement on compaction and densification behavior of Al–Al2O3 nanocomposites. Materials Science and Engineering: A. 2011;528(3):1105-10.
15. MacAskill IA, Hexemer RL, Donaldson IW, Bishop DP. Effects of magnesium, tin and nitrogen on the sintering response of aluminum powder. Journal of Materials Processing Technology. 2010;210(15):2252-60.
16. Rahmani Fard R, Akhlaghi F. Effect of extrusion temperature on the microstructure and porosity of A356-SiCp composites. Journal of Materials Processing Technology. 2007;187-188:433-6.
17. Moazami-Goudarzi M, Akhlaghi F. Effect of SiC Nanoparticles Content and Mg Addition on the Characteristics of Al/SiC Composite Powders Produced via In Situ Powder Metallurgy Method. Particulate Science and Technology. 2012;31:234-40.
18. Moazami-Goudarzi M, Akhlaghi F. Effect of Mg Content on the Characteristics of Al/SiC Nanocomposite Powders Produced via In Situ Powder Metallurgy Method. Key Engineering Materials. 2011;471-472:420-5.
19. Boettinger WJ, Kattner UR, Moon K-W, Perepezko JH. DTA AND HEAT-FLUX DSC MEASUREMENTS OF ALLOY MELTING AND FREEZING. Methods for Phase Diagram Determination: Elsevier; 2007. p. 151-221.
20. ASM Handbook, Vol. 2, Properties and selection: nonferrous alloys and special-purpose materials. USA: ASM International; 1992.
21. Shaikh MBN, Aziz T, Arif S, Ansari AH, Karagiannidis PG, Uddin M. Effect of sintering techniques on microstructural, mechanical and tribological properties of Al-SiC composites. Surfaces and Interfaces. 2020;20:100598.
22. Schaffer GB, Sercombe TB, Lumley RN. Liquid phase sintering of aluminium alloys. Materials Chemistry and Physics. 2001;67(1-3):85-91.
23. Tang F, Anderson IE, Biner SB. Solid state sintering and consolidation of Al powders and Al matrix composites. Journal of Light Metals. 2002;2(4):201-14.
24. Dabhade VV, Mohan TRR, Ramakrishnan P. Sintering behavior of titanium–titanium nitride nanocomposite powders. Journal of Alloys and Compounds. 2008;453(1-2):215-21.
25. Kondoh K, Kimura A, Watanabe R. Effect of Mg on sintering phenomenon of aluminium alloy powder particle. Powder Metallurgy. 2001;44(2):161-4.
26. Lumley RN, Sercombe TB, Schaffer GM. Surface oxide and the role of magnesium during the sintering of aluminum. Metallurgical and Materials Transactions A. 1999;30(2):457-63.
27. ASM Handbook, Vol. 3, Alloy phase diagrams. USA: ASM International; 1992.
28. Rao CS, Upadhyaya GS. 2014 and 6061 aluminium alloy-based powder metallurgy composites containing silicon carbide particles/fibres. Materials & Design. 1995;16(6):359-66.
29. Li G, Lu L, Lai MO. Liquid phase sintering of metal matrix composites. Journal of Materials Processing Technology. 1997;63(1-3):286-91.
30. Asgharzadeh H, Simchi A. Supersolidus liquid phase sintering of Al6061/SiC metal matrix composites. Powder Metallurgy. 2009;52(1):28-35.
31. Hosford WF, Caddell RM. Metal forming: Mechanics and metallurgy. 1st ed. USA: Prentice-Hall; 1983.
32. Sheppard T, McShane HB, Zaidi MA, Tan GH. The extrusion of atomised aluminium alloy compacts and composites. Journal of Mechanical Working Technology. 1983;8(1):43-70.
33. Fogagnolo JB, Robert MH, Ruiz-navas EM, Torralba JM. Extrusion of mechanically milled composite powders. Journal of Materials Science. 2002;37(21):4603-7.
34. Balog M, Simancik F, Walcher M, Rajner W, Poletti C. Extruded Al–Al2O3 composites formed in situ during consolidation of ultrafine Al powders: Effect of the powder surface area. Materials Science and Engineering: A. 2011;529:131-7.